Modeling the V_{TH} fluctuations in nanoscale Floating Gate Memories

A. Calderoni, P. Fantini, A. Ghetti and A. Marmiroli
Numonyx, R&D – Technology Development – Via Olivetti, 2 – 20041 Agrate Brianza, Italy

***Abstract*—Tight bits distribution is a must to fabricate multi-level Non-Volatile Memory (NVM) technology needed to reach a high degree of integration. On the contrary, the Non-Volatile cell shrink to nanoscale sizes produces a huge modulation in the device performances when atomistic scale fluctuations occur. The present work provides a new physically-based model allowing describing, through a simple analytical approach, the statistical V_{TH} spread for Floating Gate based NVM technologies with nanoscale dimensions.**

Keywords-component: Non-Volatile Memory; Modeling; Statistical distribution; Fluctuations; Noise.

I. INTRODUCTION

With the impressive shrinking of Non-Volatile Memory (NVM) device down to nanoscale dimensions any atomistic level fluctuation plays a significant role in the threshold voltage (V_{TH}) distribution of a memory array. However, multi-level bits storage in a single cell is a must to reach a high degree of integration and it consequently requires a better and better control of V_{TH} to get tight the bits distribution. Thus, predicting scaling limits of Flash memories on the basis of signal/noise ratio requires both physical models and the analysis of the statistical distributions of the cell threshold voltage [1]. Definitively, fluctuations in general, could become a strong concern in the next generation NVM technologies. This paper deals with the problem of threshold voltage fluctuations due to the Discrete Dopant Effects (DDE) but also introducing the Non-Uniform Conduction concept (NUC), including the Edge Effects (EE), the Trap and oxide fixed charge Distribution (TD) with the related Random Telegraph Signal (RTS) for a nanoscale Flash memory array. The capability to capture the relevant physical phenomena and their own weight with a simple analytical approach appears a strength point of the model otherwise supported by a physical understanding [2]. The resulting bit distributions are compared against experimental data and a good agreement in between is found. This further allows shedding some light on the scaling perspectives.

II. EXPERIMENTAL

Bit distribution in 65 nm NOR-like Flash memory arrays has been extensively characterized. However, in order to compare our physically based model with 'intrinsic' threshold distribution, a half Mbit array of equivalent transistors has been designed and measured. So, the V_{TH} differences due to different amount of Floating gate charge could be deleted, otherwise maintaining the memory array topology. Threshold measurements were performed at a defined current as in the real memory chip. Also the distribution of V_{TH} differences between two consecutive measurements has been considered in order to capture the role of RTS phenomena becoming more and more important with the cell area scaling down.

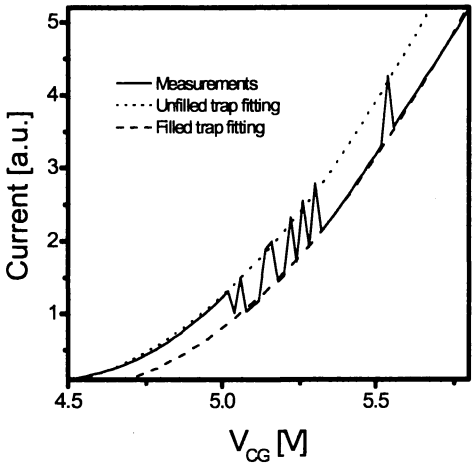

Figure 1. The transfer curve of a Flash cell affected by RTS phenomenon well fitted in strong inversion by means of (1) (see text) for both empty and filled trap state.

III. STATISTICAL MODEL FOR V_{TH} FLUCTUATIONS

The basis of the model starts from the experimental observation that the transfer *I-V* curve of a single cell in reading condition can be well pictured by the simple and well-known classical formula:

$$I_D = \frac{1}{2}\mu_{eff}\frac{\varepsilon_{OX}}{T_{OX}}\left(\frac{w}{l}\right)_{eff}\cdot\left(V_{CG}-V_{TH}\right)^2 \qquad (1)$$

being μ_{eff} the effective carrier mobility, ε_{ox} the SiO_2 dielectric constant, T_{ox} the oxide thickness, w_{eff} and l_{eff} the effective width and length of the cell, V_{CG} the control gate bias. This simple equation well describes the cell transfer curve beneath the decananometer device dimensions and also when RTS phenomena affecting its performance, see Fig. 1 [3].
We solve (1) with respect to the Control Gate bias (V_{CG}) considering a fixed threshold current, in agreement with the definition of the threshold voltage measured at chip level:

$$V_{CG} = V_{TH} + \sqrt{\frac{2I_D}{\mu_{eff}}\frac{T_{OX}}{\varepsilon_{OX}}\left(\frac{l}{w}\right)_{eff}} \qquad (2)$$

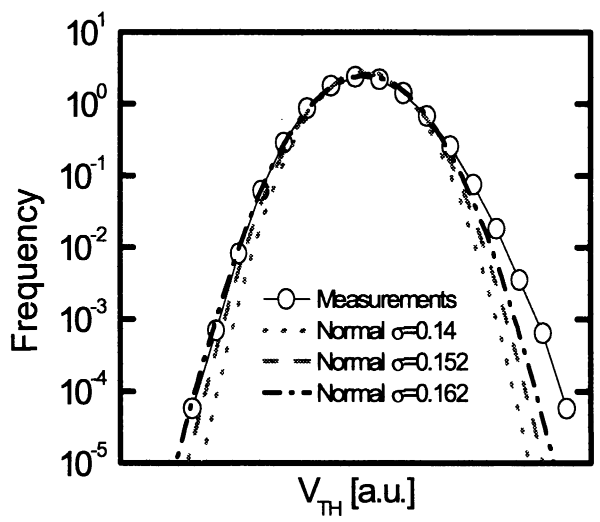

Figure 2. Measurements/simulation comparison of the 'intrinsic' VTH distribution of a 512 Kbits dummy cells array. The switching on, step-by-step, of each contribution DD (cont. line), geometrical fluctuations (dashed-line), and oxide fixed traps (dashed-dot line) is reported up to obtain a satisfactory agreement with the experimental spread.

Then, we switch on step by step any contribution to statistical fluctuation of the physical V_{TH} described through a compact-like expression:

$$V_{TH} = V_{TH0} + f(w_{eff}, l_{eff}) \qquad (3)$$

Where V_{TH0} represents the threshold voltage term depending on channel doping, oxide thickness and oxide fixed charge, while $f(w_{eff}, l_{eff})$ is the scaling function picturing the V_{TH} roll-on/roll-off correlated to the geometry fluctuation. Both terms are defined with compact-like expression resembling the BSIM model.

First of all, we introduce the role of discrete dopant fluctuations that, on the basis of accurate numerical simulations and against a simplified picture, scales the sigma of V_{TH} as $N_D^{0.4}$ and the inverse of the square root of area device [4]. Then, we give out randomly generated Montecarlo-like proofs describing the discrete dopant fluctuations in the threshold expression. A tighter distribution than the experimental one can be observed, see the continuous line in Fig. 2. So, we added in

$$I_D = \sum_{i=1}^{N} I_{Di}$$

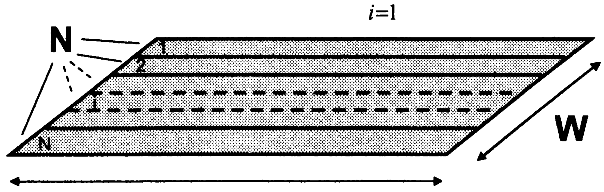

Figure 3. Schematic picture of the channel as it was composed by a number of slices of conducting paths in parallel to account for the NUC effect (see text). Equation reports the current expressed as the sum of the current of each channel slice.

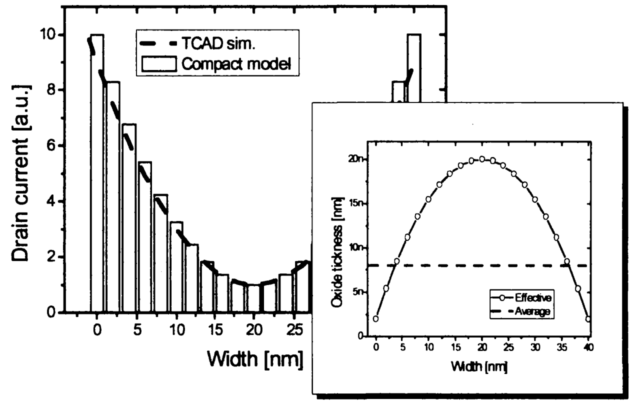

Figure 4. Modeling a 'virtual' T_{OX} modulation along the cell width (right side)in order to take into account for the corner effect promoting there a current crowding matching the TCAD simulation current density (left side). T_{OX} quadratic function's parameters are calculated to obtain an average T_{OX} value corresponding to the physical oxide thickness.

the picture described by the compact-like expression for V_{TH} also the random geometrical fluctuation (by technology on such an array) with the correlated impact in the threshold roll-off effect. With a new Montecarlo iteration we approached the experimental distribution, but not yet completely (see dashed-line in Fig. 2). If we consider that also oxide fixed charge presence can fluctuate [5] and we add this further term (Q_{OX}/C_{OX}) in (3) a nice fitting with the intrinsic distribution is observed (Fig. 2, dot-dashed line).

Then, we introduced Non-Uniform Conduction (NUC) effects that play a role in the RTS-induced V_{TH} fluctuations [2,3,6]. To this aim and in order to keep "compact" the model we describe local effects dividing our device in a number of slices as shown in Fig. 3 and the inserted equation.

Here below, we summarize any spread contribution included in our model with their modeling issues:

a) Edge effects: the active area corner enhances the lateral electrical field. We have modelled this effect by using a quadratic function of T_{OX} describing an "effective" oxide thickness thinning, inducing a current crowding close to the AA edges, as well simulated by using TCAD tools (Fig. 4). T_{OX} quadratic function's parameters are calculated to obtain an average T_{OX} value corresponding to the physical oxide thickness.

b) Discrete Dopant Effects: in addition with a gaussian V_{TH} spread which amplitude is calibrated by Montecarlo-generated cases varying number and positioning of dopants via atomistic 3D-TCAD simulations [2,4], as for 'intrinsic' V_{TH} fluctuations, we assume that Boron ions inhibit the current flow in a certain percentage (model parameter) of the channel width. A current crowding obtained by increasing mobility in the nearby slices is assumed (Fig. 5).

c) Statistical distribution of traps: a uniform spatial distribution of traps has been imposed with a trap density $\sim 1e^{10}/cm^2$ accordingly the 1/f like noise Spectral Density dependence captured by averaging on a large number of devices (Fig. 6).

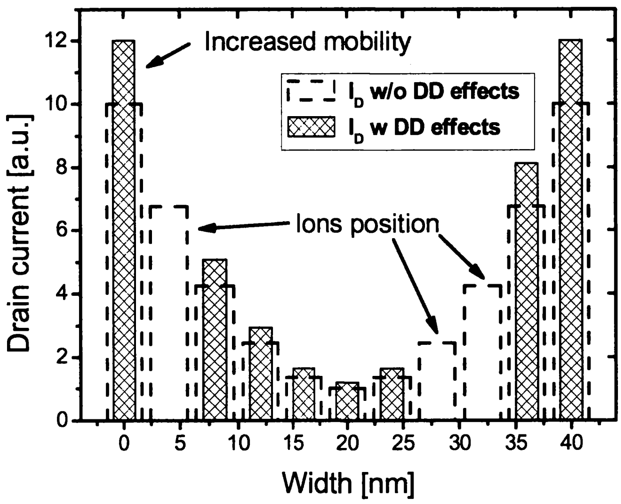

Figure 5. Modeling the *DD* effects from Montecarlo runs on various dopants distribution and the Non Uniform Conduction.

d) Random Telegraph Signal: it has been introduced through a local variation of the threshold voltage due to trapping/detrapping events in agreement with what reported in [2].

The ΔV_{TH} due to the channel loss of one electron captured by a trap is:

$$\Delta V_{TH} \approx \frac{q}{C_{OX} S} \tag{2}$$

where S is the trap interaction area fixed equal to the Debye length for a two-dimensional electron gas with the appropriate doping ($L_D \sim 4$ nm). In this way, we can describe the RTS amplitude larger than in (2) because of the strategically positioned trap along with the high current density filament.

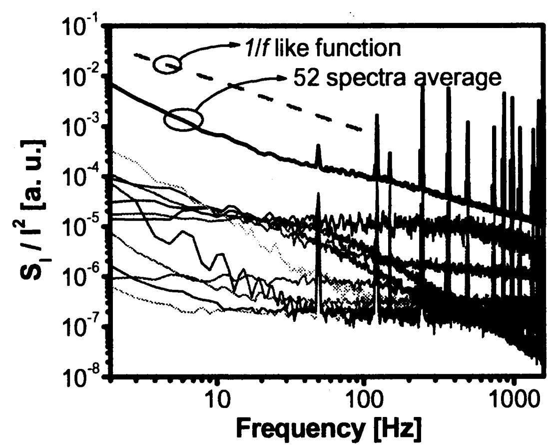

Figure 6. Measurement of Noise Spectral Density of 65nm Flash memmory cells. The upper spectrum represents the curve obtained by averaging 52 measurements that resembles the 1/f noise.

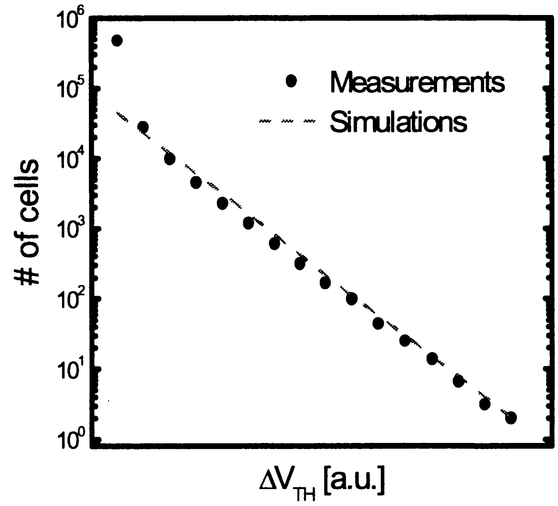

Figure 7. Measurements/simulation comparison of the RTS-induced ΔV_{TH} distribution of a 512 Kbits dummy cells array. The proposed 'channel sliced' compact model well reproduces the experimental distribution slope.

Within this framework, the RTS-induced ΔV_{TH} distribution in half Mbits array of dummy cells is due to the overall aforementioned contributes together with the dispersion of geometrical values given by technological charts. Fig. 7 shows the simulations result obtained by using the proposed model in comparison with the experimental distribution. An excellent capability of our model to capture the experimental slope can be observed.

IV. Scaling Perspectives

Our model, through the Non-Uniform Conduction concept in the W direction, suggests that width and length are non-homologous sizes. We suggest that this concept drives the scaling rule of V_{TH} fluctuations. In particular, we observe that ΔV_{TH} due to RTS does not scales with the inverse of cell area (Fig. 8). This can be explained by introducing a novel term adding to the Asenov's term [4] taking into account for also the combination with NUC effects (EE and DDE) and the 'strategically' located trap probability along with the W of the cell. Each of them scales with $1/\sqrt{W}$, assuming Poissonian distributions. Then:

$$\sigma_{\Delta V_{TH}} \propto \frac{N_D^{0.4}}{\sqrt{W \cdot L}} \cdot \frac{1}{W^{3/2}} \tag{3}$$

Definitely, our model predicts that cell width plays more and more an important role in the RTS-induced V_{TH} fluctuation and then, the AA corner shape and the doping concentration must be strongly controlled to minimize the NUC effects. This model also captures the recently reported experimental findings [6].

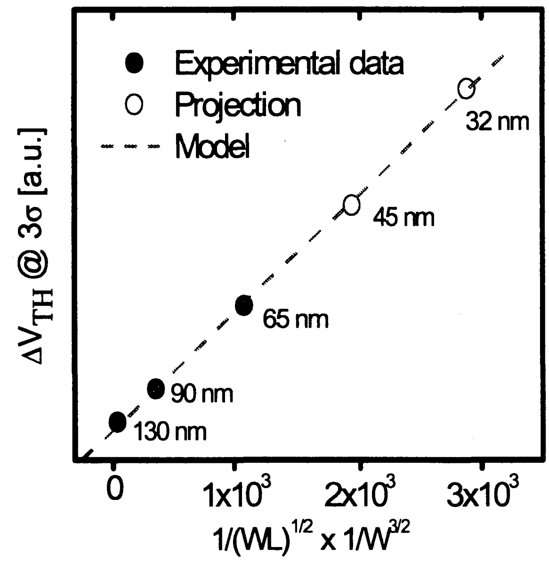

Figure 8. ΔV_{TH} @ 3-σ of the RTS-induced distribution as a function of cell geometrical parameters and the respective technology node. Filled-dots are experimental data empty-dots and dashed lines are the projections of our model distribution slope.

V. Conclusions

We have presented an analytical model that is able to describe the nanoscale V_{TH} fluctuations that are potential sources of read fail of a Flash memory. It well pictures both the 'intrinsic' experimental spread and the RTS distribution of a consolidate technology. Then, projections on the next generation technologies have been addressed finding out that the cell width, the AA corner shape and the channel doping concentration represent key factors in determining the memory cell V_{TH} fluctuations beyond the 65 nm technology node [7].

References

[1] R. Gusmeroli et al., IEDM Tech Dig., p. 483, 2006.

[2] A. Ghetti et al., IRPS Proc., p. 610, 2008.

[3] P. Fantini et al., Electr. Dev. Lett., 28, 1114-1116 (2007).

[4] A. Asenov et al., Tran. Electr. Dev. 50, 839-845 (2003).

[5] Muller and Shultz, J. Appl. Phys. 79, 4178-4180 (1996).

[6] R. Lu et al., VLSI, p. 85, 2008.

[7] A. Asenov et al., IEEE Elect. Dev. Let., vol. 29 (2008).